analytical chemistry

pubs.acs.org/ac

Article

Sensing ATP: Zeolitic Imidazolate Framework-67 Is Superior to Aptamers for Target Recognition

Zhen Wang, Xumei Zhou, Yuqing Li, Zhicheng Huang, Jing Han, Gang Xie,* and Juewen Liu*

Cite This: *Anal. Chem.* 2021, 93, 7707−7713

Read Online

ACCESS | Metrics & More | Article Recommendations | Supporting Information

ABSTRACT: In a typical biosensor, a biomolecule such as an aptamer is used for target recognition, and a nanomaterial is used for signal generation. Herein, we communicate a reverse system using a nanomaterial for target recognition and a DNA for signaling. We discovered that a classic metal−organic framework material, zeolitic imidazolate framework (ZIF)-67, has ultrahigh selectivity for recognizing adenosine triphosphate (ATP), allowing a fluorescently labeled DNA oligonucleotide to be used for signal generation. This sensor showed up to a 24-fold increase in fluorescence upon adding 1 mM ATP, while the fluorescence increase after adding adenosine or guanosine triphosphate was less than twofold. Its selectivity is much better than that of the ATP aptamer, which binds adenosine even better. Using isothermal titration calorimetry, the selective binding of ATP was independently verified. This sensor has a detection limit of 29 nM ATP and it can even detect ATP in serum. By replacing Co^{2+} with Zn^{2+} to form ZIF-8 or by using CoO, the selectivity for ATP was lost. Therefore, by sophisticated material design, ultrahigh selectivity for molecular recognition can be achieved.

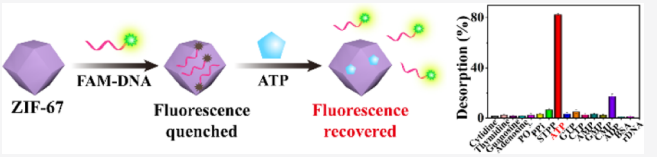

INTRODUCTION

Biosensors are typically constructed by using biological ligands such as antibodies and aptamers for target recognition, whereas nanomaterials have been increasingly used for signal transduction.[1−4] Interestingly, nanomaterials can also be used for target recognition. For example, a Fe_3O_4/DNA conjugate was used for the detection of arsenate, taking advantage of the strong adsorption of arsenate to Fe_3O_4 to displace DNA.[5] Similarly, CeO_2/DNA was able to detect H_2O_2 due to the strong adsorption of H_2O_2 to CeO_2.[6] A general perception is that biological ligands have better selectivity since many molecules may have similar adsorption affinities to nanomaterials. Nevertheless, nanomaterials can have sophisticated structures as well, and we wonder whether they can also possess exquisite molecular recognition functions.

Metal−organic frameworks (MOFs) are a powerful platform to rationally design nanomaterials.[7] Zeolitic imidazolate frameworks (ZIFs) are a popular class of MOFs due to their facile synthesis and good chemical stability.[8] ZIF-8 and ZIF-67 are formed by the coordination of 2-methylimidazole (2-MI) with Zn^{2+} and Co^{2+}, respectively, and have been exploited for various applications ranging from drug delivery and catalysis to bioanalysis.[9−13]

Adenosine triphosphate (ATP) is the primary energy currency in biology. Many analytical methods such as electrochemistry,[14] electrochemiluminescence,[15] surface enhanced Raman scattering,[16] colorimetry,[17] and fluorimetry[18,19] have been developed for ATP detection.[20−23] Most of these ATP biosensors relied on an aptamer, which can hardly differentiate ATP from adenosine monophosphate (AMP) or adenosine.[24] In addition, most small molecular probes for ATP require multistep synthesis, yet they also have a poor selectivity for ATP over adenosine diphosphate (ADP).[25,26] Herein, we communicate that ZIF-67 has exceptional affinity and specificity for adsorbing ATP, allowing us to design a simple fluorescent sensor, exceeding the aptamer in both selectivity and sensitivity.

EXPERIMENTAL SECTION

Chemicals. All the DNA samples were purchased from Integrated DNA Technologies (IDT, Coralville, IA, USA), and the sequences are listed in Table S1. Zinc nitrate [$Zn(NO_3)_2$], cobalt(II) nitrate [$Co(NO_3)_2$], 2-MI, thioflavin T (ThT), AMP, guanosine monophosphate, cytidine monophosphate, ADP, ATP, guanosine triphosphate (GTP), cytidine triphosphate (CTP), sodium triphosphate (STPP), CoO nanoparticles, ZnO nanoparticles, bovine serum albumin (BSA), and fetal bovine serum (FBS) were purchased from Sigma-Aldrich. Carboxyl graphene oxide (GO) was purchased from ACS Material (Medford, MA). 4-(2-Hydroxyethyl)piperazine-1-ethane sulfonate (HEPES) and the four nucleosides were obtained from Mandel Scientific (Guelph, Ontario, Canada). Milli-Q water was used to prepare buffers and solutions.

Received: March 4, 2021
Accepted: May 3, 2021
Published: May 17, 2021

https://doi.org/10.1021/acs.analchem.1c00976
Anal. Chem. 2021, 93, 7707−7713

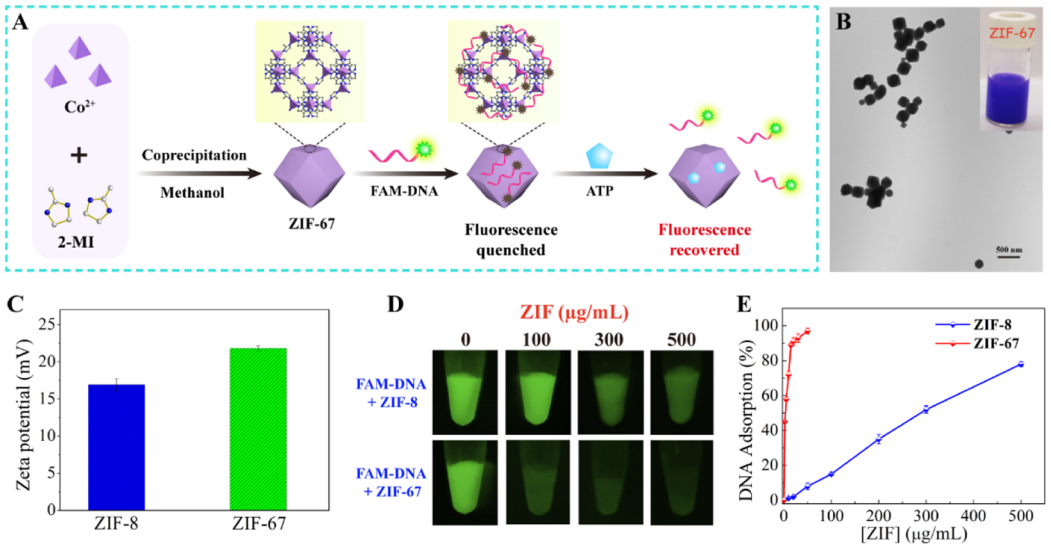

Figure 1. (A) Schematic illustration of the co-precipitation synthesis of ZIF-67 and fabrication of the fluorescence biosensor for ATP detection. (B) A TEM image of ZIF-67 (inset: a photograph of 4 mg/mL ZIF-67 dispersed in HEPES buffer). Scale bar: 500 nm. (C) ζ-Potentials of ZIF-8 and ZIF-67. (D) Fluorescence photographs of free FAM-12mer (100 nM) after adding different concentrations of ZIF-8 and ZIF-67. (E) Adsorption efficiencies of FAM-12mer (10 nM) by varying the concentration of ZIF-8 and ZIF-67. Each measurement was repeated 3 times and the error bars represent one time of the standard variation.

Apparatus and Characterization. ζ-Potential was measured using dynamic light scattering (Zetasizer Nano 90, Malvern). The morphologies and structural analysis of ZIF-8 (Zn) and ZIF-67 (Co) were carried out by a transmission electron microscope (Philips CM10 100 kV microscope), powder X-ray diffractometer (Bruker D8), and X-ray photoelectron spectroscope (PerkinElmer). Fourier transform infrared (FT-IR) spectra were recorded with a Tensor 27 spectrometer (Bruker Optics, Ettlingen, Germany) with KBr pellets in the range of 4000−400 cm^{-1}. The fluorescent intensity was recorded on a microplate reader (Infinite F200 Pro, Tecan) with excitation at 485 nm and emission at 535 nm.

Synthesis of ZIF-8 and ZIF-67. ZIF-8 (Zn) and ZIF-67 (Co) were prepared according to previous literature.[27] Typically, 0.5 mmol $Zn(NO_3)_2$ or $Co(NO_3)_2$ and 4 mmol 2-methylimidazole were separately dissolved in 7 mL of methanol. Subsequently, the 2-methylimidazole solution was added into the $Zn(NO_3)_2$ or $Co(NO_3)_2$ solution rapidly and incubated for 24 h at room temperature. Finally, the products were collected by centrifugation, washed with methanol, and then dried overnight at 60 °C.

DNA Adsorption Capability and Kinetics. In a typical experiment, 10 μL of ZIF-8 or ZIF-67 was mixed with 90 μL of 10 nM FAM-12mer DNA in HEPES buffer (10 mM, pH 7.6) and incubated for 30 min. After centrifugation at 15,000 rpm, the fluorescence intensity of the supernatant (containing non-adsorbed DNA) was recorded using a microplate reader with excitation at 485 nm and emission at 535 nm. To measure DNA adsorption kinetics, the background fluorescence was first collected from 95 μL of the FAM-12mer (10 nM) in 10 mM HEPES buffer (pH 7.6) for 5 min. After that, 5 μL of ZIF-8 or ZIF-67 was added, and the fluorescence intensity was monitored for 30 min.

DNA Desorption. DNA desorption was studied by following the fluorescence increase after adding various competing agents to the FAM-12mer/ZIF-8 and FAM-12mer/ZIF-67 conjugates. Typically, 10 nM FAM-12mer was first mixed with 500 μg/mL ZIF-8 or 50 μg/mL ZIF-67 in HEPES buffer (10 mM, pH 7.6) and then incubated for 30 min. Different competing molecules were subsequently introduced to the above conjugates. After another 60 min of incubation followed by centrifugation, the fluorescence of the supernatant indicative of desorbed DNA was measured. For comparison, the DNA displacement experiments were also performed for the ZnO and CoO conjugates.

ThT Fluorescence Spectroscopy. To test the binding of the adenosine aptamer toward different analytes, 200 μM of target molecules was first mixed with 300 nM of the aptamer in HEPES buffer (10 mM, pH 7.6) containing 2 mM $MgCl_2$ and incubated for 20 min. Subsequently, 8 μM ThT was introduced, and the fluorescence intensity was recorded after 5 min using a microplate reader with excitation at 420 nm and emission at 500 nm.

Isothermal Titration Calorimetry. Isothermal titration calorimetry (ITC) was performed using a VP-ITC microcalorimeter instrument (MicroCal). Prior to the measurement, each sample was degassed to eliminate air bubbles. Typically, 2.6 mM ZIF-67 in HEPES buffer (20 mM, pH 7.6) was loaded in a 1.45 mL ITC cell at 25 °C. Then, 280 μL of 0.5 mM various molecules (ATP, ADP, AMP, adenosine, or STPP) in the same buffer was respectively titrated into the cell *via* a syringe with 10 μL each time, except for the first injection of 2 μL. The time-dependent heat changes were integrated for analysis.

Determination of ATP. The ATP biosensor was prepared by adsorbing 10 nM FAM-12mer onto 50 μg/mL ZIF-67 in HEPES buffer (10 mM, pH 7.6). Afterward, ATP solutions of varying concentrations were added into the sensor dispersion at room temperature to release FAM-12mer, where DNA desorption was studied by monitoring the kinetics of fluorescence increase. The signal was quantified by calculating the fluorescence enhancement factor $F/F_0 - 1$, where F_0 and F represent the fluorescence of the assay in the absence and presence of ATP, respectively.

ATP Sensing in Diluted Serum. For sensing ATP in FBS, 1% FBS was prepared by diluting the serum sample in 10 mM

https://doi.org/10.1021/acs.analchem.1c00976
Anal. Chem. 2021, 93, 7707−7713

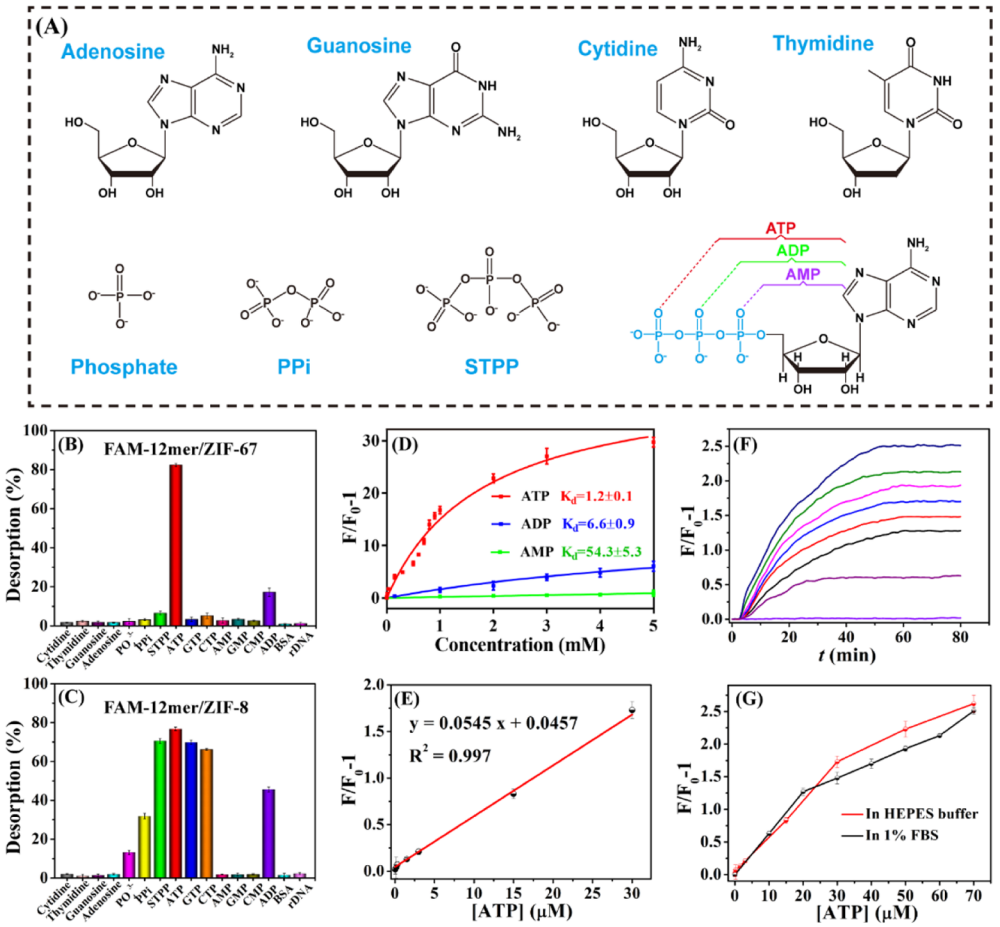

Figure 2. (A) Structures of various nucleobases (adenosine, guanosine, cytidine, and thymidine) and phosphate-containing species tested in this work. Desorption efficiencies of FAM-12mer DNA (10 nM) from (B) 50 μg/mL ZIF-67 and (C) 500 μg/mL ZIF-8 induced by different competing molecules after 100 min incubation (nucleosides: 10 mM; other species: 1 mM). (D) Relative fluorescence enhancement of FAM-12mer (10 nM) from ZIF-67 (50 μg/mL) induced by different concentrations of ATP, ADP and AMP. (E) Linearly fitted relationship in the low concentration range up to 30 μM. (F) Kinetics of fluorescent recovery and (G) relative fluorescence enhancement of FAM-12mer (10 nM) from 50 μg/mL ZIF-67 induced by different concentrations of ATP in 1% FBS. Each measurement was repeated 3 times.

HEPES (pH 7.6). Then, ATPs of varying concentrations were spiked into the 1% FBS in the presence of the FAM-12mer/ZIF-67 conjugates, and the kinetics of fluorescence recovery were monitored.

RESULTS AND DISCUSSION

ZIF-67 Adsorbs DNA Efficiently. ZIF-67 was prepared using a co-precipitation method by mixing 2-methylimidazole and Co^{2+} in methanol (Figure 1A, step 1). The purple product appeared to be hexagonal particles of ~200 nm under TEM (Figure 1B and inset). For comparison, 50 nm ZIF-8 was prepared using Zn^{2+} in place of Co^{2+}, giving it a milky color (Figure S1). The structures of ZIF-8 and ZIF-67 were confirmed by powder X-ray diffraction (Figure S2) and FT-IR spectroscopy (Figure S3). In water, both materials had a positive surface charge (Figure 1C) and thus were expected to adsorb negatively charged DNA.

Indeed, when ZIF-8 and ZIF-67 were added to a FAM (6-carboxyfluorescein)-labeled 12mer DNA (named FAM-12mer), quenched fluorescence was observed (Figure 1D), suggesting DNA adsorption (Figure 1A, step 2). Interestingly, the fluorescence quenching by ZIF-67 was much stronger than that by ZIF-8. To quantitatively characterize DNA adsorption, the FAM-12mer (10 nM) was then mixed with various concentrations of ZIF-8 or ZIF-67 in HEPES buffer. After centrifugation, the fluorescence intensity retained in the supernatant was measured to quantify DNA adsorption efficiency (Figure 1E). To reach 50% adsorption, 300 μg/mL of ZIF-8 was needed, whereas only 2 μg/mL was required for ZIF-67, indicating that the ZIF-67 was around 150-fold more efficient in DNA adsorption, despite ZIF-67's larger particle size (and thus a less specific surface area). ZIF-67 also had faster DNA adsorption kinetics (Figure S4).

ZIF-67 Is Highly Selective for ATP. After achieving DNA adsorption, we then added various molecules as competitors to desorb the DNA, which would be accompanied by fluorescence enhancement (Figure 1A, step 3). Since DNA is composed of nucleosides and phosphate, we focused on them as competing molecules (Figure 2A). Among four types of nucleosides (adenosine, thymidine, cytidine, and guanosine), various phosphates (orthophosphate, pyrophosphate, and triphosphate), and nucleoside mono-, di-, and triphosphates, only ATP gave a high fluorescence signal for the FAM-12mer/ZIF-67 sample (Figure 2B). The next highest signal from ADP was 4.8-fold lower, while AMP had only a background level of response. In addition, no response was observed from other nucleoside triphosphates, such as GTP and CTP. Since this 12-mer DNA is not an aptamer for ATP, its desorption was

https://doi.org/10.1021/acs.analchem.1c00976
Anal. Chem. 2021, 93, 7707−7713

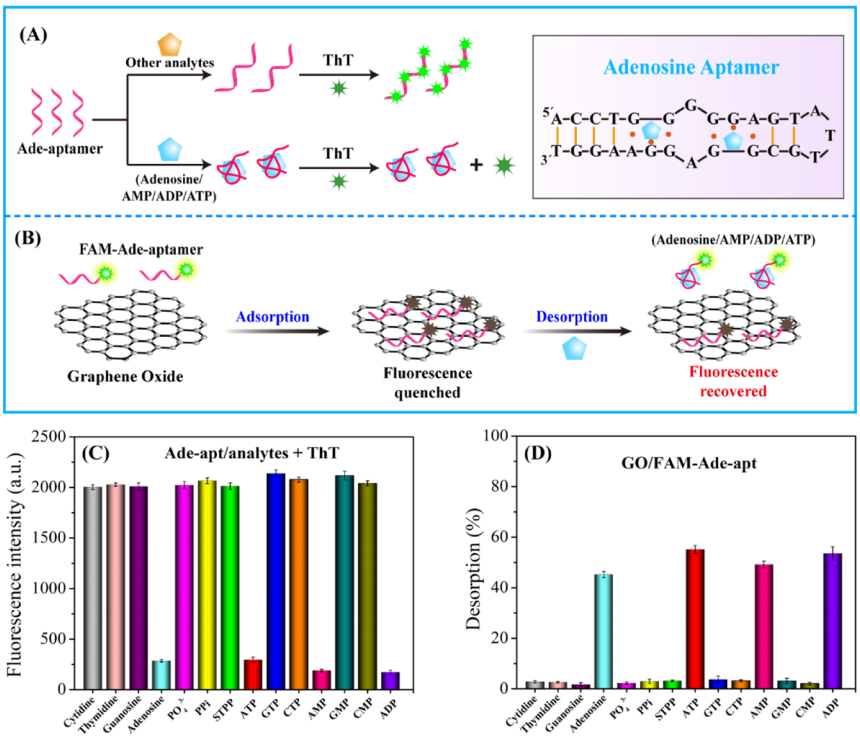

Figure 3. (A) ThT fluorescence spectroscopy for testing the binding of the aptamer and the secondary structure of adenosine aptamer. (B) Scheme for adsorption of the FAM-labeled adenosine aptamer on GO for detecting ATP. (C) Binding of the adenosine aptamer toward different analytes measured using ThT. (D) Desorption efficiencies of the FAM-Ade-aptamer (10 nM) from GO (3 μg/mL) induced by 1 mM of various analytes. Each measurement was repeated 3 times.

attributed to competitive ATP adsorption. Therefore, ZIF-67 might specifically recognize ATP on its nucleobase and its triphosphate at the same time.

When the Zn^{2+}-based ZIF-8 was used to adsorb the FAM-12mer, the fluorescence response had no obvious selectivity (Figure 2C). It appeared that the more phosphate units a molecule had, the more fluorescence enhancement it achieved, suggesting that the FAM-12mer might use its phosphate backbone to interact with ZIF-8. On the other hand, both the phosphate backbone and adenine interacted with ZIF-67, with each interaction being very strong. Only when ATP was added to compete for both interactions can DNA desorption be achieved. From the relative fluorescence enhancement induced by different concentrations of ATP, ADP, and AMP (Figures 2D and S5), the apparent dissociation constants (K_d) were calculated to be 1.2 mM ATP, 6.6 mM ADP, and 54.3 mM AMP, indicating the strongest affinity was to ATP. The saturated fluorescence enhancement by ATP reached nearly 30-fold, suggesting this system can be a highly sensitive and selective biosensor for detecting ATP.

To confirm that adenosine had a higher affinity compared to other nucleosides, we added increasing concentrations of the nucleosides (Figure S6). When the concentration of adenosine reached 20 mM, about 20% of the DNA desorbed, but no DNA desorption was observed with thymidine, guanosine, or cytidine. Therefore, the adenine base indeed played an important role for inducing DNA desorption.

The kinetics of fluorescence increase from ZIF-67 were quite fast and more than 50% of the adsorbed DNA strands were desorbed by ATP within 10 min (Figure S7). Finally, BSA as well as a 12-mer random DNA were also added, but neither desorbed the FAM-12mer from ZIF-67, suggesting that this system was highly robust and can resist interference from biological sample matrices (Figure S8).

Both 2-Methylimidazole and Co^{2+} Are Required. To understand the mechanism of such high specific ATP recognition, we then respectively adsorbed the FAM-12mer onto ZnO and CoO nanoparticles (Figure S9). When challenged with the same small molecules, FAM-12mer desorption from CoO occurred most with STPP, while ATP showed a lower response (Figure S9A). Since ZIF-67 and CoO had the same metal ion (the Co^{2+} in ZIF-67 was confirmed by XPS spectra in Figure S10), the change of the metal ligand from oxygen to 2-methylimidazole was critical for the specific recognition of ATP by ZIF-67. 2-Methylimidazole is a larger ligand that can produce a longer ligand-bridged Co^{2+}-to-Co^{2+} distance (6 Å) compared to that in CoO (4.3 Å). According to the crystal structures (Figure S11), each cobalt atom in ZIF-67 is coordinated with four nitrogen atoms, while CoO has a cubic NaCl crystal structure with each Co^{2+} ion coordinated by six oxygen atoms. The longer Co^{2+}-to-Co^{2+} distance might be more compatible with the distance between the non-bridging oxygen atoms in the triphosphate, while the coordination unsaturated Co^{2+} on the surface of ZIF-67 may bind more strongly with the nitrogen atoms in adenine. Similarly, by comparing ZIF-67 and ZIF-8, we concluded that Co^{2+} can interact with DNA more strongly than Zn^{2+}, with this conclusion also being supported by comparing DNA desorption from ZnO and CoO.

For metallic nanoparticles (*e.g.*, AuNPs)[28] and carbon-based nanomaterials (*e.g.*, graphene oxide),[29] DNA adsorption is achieved *via* base interaction, while many metal oxide nanoparticles (*e.g.*, CeO_2, Fe_3O_4, ZnO) adsorb DNA mainly *via* the phosphate backbone.[30−32] On ZIF-67, both adenine

https://doi.org/10.1021/acs.analchem.1c00976
Anal. Chem. 2021, 93, 7707−7713

Table 1. Some Literature Reported Sensors for ATP Detection and the Relative Signal for Adenosine, AMP, ADP, ATP, and GTP[a]

	response molecule					
recognition probe	adenosine	AMP	ADP	ATP	GTP	references
aptamer−Ru(II)		0.57[b]	0.93[b]	1[b]		1[39]
zinc complex	0.89[c]	0.06[c]	0.08[c]	1[c]		2[40]
zinc complex		1.08[c]	0.97[c]	1[c]		3[41]
zinc complex		0.22[c]	0.77[c]	1[c]		4[42]
zinc complex			1.06[c]	1[c]	1.09[c]	5[43]
europium complex		0.77[d]	1.05[d]	1[d]		6[44]
bis[Zn(II)DPA]			0.03[d]	1[d]	1[d]	7[45]
ZIF-67 (Co)	0.02[c]	0.03[c]	0.21[c]	1[c]	0.04[c]	this work

[a]The values in the table are the ratio of the analogues to ATP. [b]The numbers in the table are compared to ATP based on luminescence intensity. [c]The numbers in the table are compared to ATP based on fluorescence intensity. [d]The numbers in the table are compared to ATP based on association constants (log K_a).

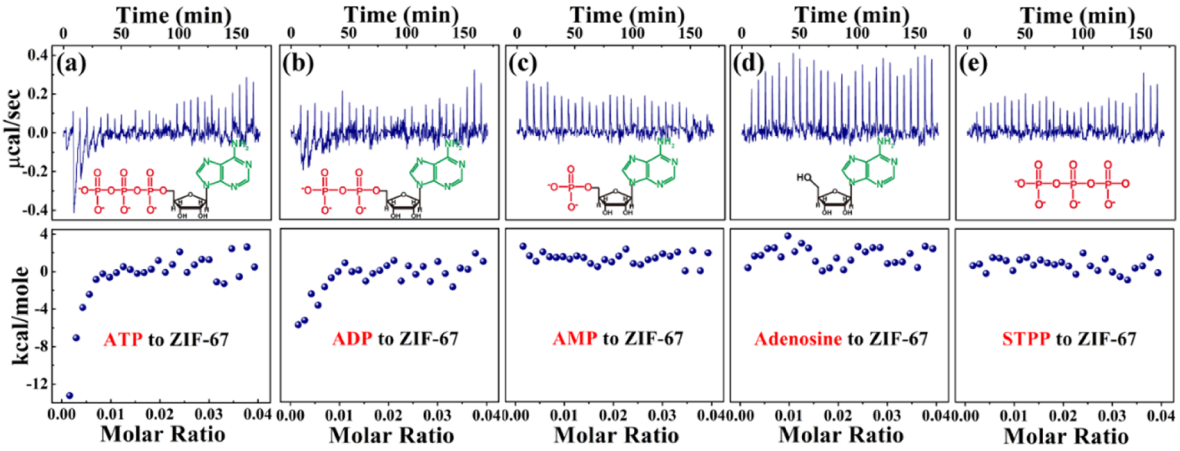

Figure 4. ITC traces (top) and the integrated heat (bottom) of titrating 0.5 mM (a) ATP, (b) ADP, (c) AMP, (d) adenosine, and (e) STPP into 2.6 mM ZIF-67 (based on the total Co^{2+} concentration) in HEPES buffer (20 mM, pH 7.6).

and phosphate contributed to the adsorption, leading to excellent selectivity for ATP.

Better Selectivity than the ATP Aptamer. The majority of previous DNA-based detection of ATP molecules relied on a 27-mer aptamer (Figure 3A).[33] To compare its selectivity with our ZIF-67, we measured the binding of the aptamer toward different analytes using ThT as a staining dye.[34] Specific binding of ATP is expected to displace ThT from the aptamer, resulting in quenched fluorescence. As shown in Figure 3C, all four adenosine-containing molecules induced more than an 85% fluorescence decrease, while the other analytes had little signal change. This was consistent with the expected selectivity of this aptamer to recognize adenosine but not the phosphate part.[35,36]

For further comparison, we adsorbed the FAM-labeled aptamer on GO and tested the desorption efficiency with the addition of different competing agents (Figure 3B).[37,38] Although this sensor was also based on DNA desorption, its target recognition relied on the aptamer, while for the above ZIF-67, the recognition was based on ZIF-67. When 1 mM of each species was respectively added to the GO samples, a fluorescence increase was observed in all the adenosine-containing compounds (Figures 3D and S12). Therefore, ZIF-67 enabled much higher selectivity for ATP than the classic aptamer.

Furthermore, a series of other literature-reported complexes and ATP aptamers as recognition probes for ATP detection are compared in Table 1. The majority of these complexes bind AMP, ADP, and ATP with similar affinities and produce similar signal responses. Thus, ZIF-67 exhibited superior selectivity for ATP, which may benefit from the strong interaction of its adenine base and its triphosphate at the same time. Since there are so many examples of biosensors based on the aptamer,[36] we did not include most of them in this table. They all inevitably suffer from interference from ADP, AMP, or adenosine, exhibiting a poor selectivity for ATP. In contrast, ZIF-67 exhibited a strong affinity and fast response for discriminating ATP against other molecules even in biological sample matrices.

Selective ATP Binding Confirmed by ITC. The above experiments were all performed using competitive DNA displacement assay with fluorescence spectroscopy. To have a direct measurement of ATP adsorption, we also followed the reaction using ITC.[46−48] Titration of the buffer to ZIF-67 was used as the background, which was subtracted from each sample heat. As shown in Figure 4a, the titration of ATP into ZIF-67 showed most heat release, consistent with the strongest binding. We then tested ADP (Figure 4b), but the heat release was much lower than that of ATP, indicating a weaker binding. AMP, adenosine, and STPP (Figure 4c−e), however, showed no significant binding to ZIF-67, which was consistent with the fluorescence data. Therefore, the ITC results verified the highest affinity between ATP and ZIF-67. Due to the limited surface area of nanomaterials, the ITC signals here were

https://doi.org/10.1021/acs.analchem.1c00976
Anal. Chem. 2021, 93, 7707−7713

relatively weak, which was also observed in the titration of other nanomaterials such as gold nanoparticles[49] and graphene oxide.[50] As such, no quantitative fitting was performed, and ITC only served as an independent verification of the specific binding between ATP and ZIF-67.

Highly Sensitive Detection of ATP. Encouraged by the enormous fluorescence enhancement brought by ATP, we then evaluated the sensitivity of FAM-12mer/ZIF-67 for the detection of ATP. The fluorescence enhancement ($F/F_0 - 1$) increased gradually with increasing ATP concentration (Figure 2D, red trace). Figure 2E presents a good linear correlation in the low concentration range from 0.03 to 30 μM. The limit of detection was determined to be 29 nM based on the 3σ/slope, where σ is the standard deviation of background fluorescence variation. Such sensitivity also compared favorably to aptamer-based ATP detection without signal amplification where the detection limits were often in the low micromolar region.[51,52]

Assay of ATP in Diluted Serum. To demonstrate the potential analytical application in a real sample, a quantitative ATP detection experiment was performed in 1% FBS. As shown in Figure 2F,G, upon the addition of various concentrations of ATP, the quenched fluorescence of FAM-12mer by ZIF-67 increased gradually. The fluorescence recovery in the diluted FBS was close to that in the clean buffer, which indicated that the proteins or other molecules in the serum did not interfere with the sensor. Thus, this sensor has excellent potential for ATP determination in real biological samples.

CONCLUSIONS

In conclusion, this work has presented an example to use nanomaterials for highly selective target recognition and use biomolecules for signal generation, which is opposite to the design of typical biosensors. We discovered that ZIF-67 had exceptional affinity and specificity for adsorbing ATP. ZIF-67 not only fully discriminated against other nucleoside triphosphates but also had 4.8-fold higher selectivity against ADP. The sensitivity and selectivity were both much better than the sensors made using the classic ATP aptamer. Given the versatility of MOF design by tuning both metal ions and organic ligands, highly selective recognition of other important target molecules might also be achieved using this strategy.

ASSOCIATED CONTENT

Supporting Information

The Supporting Information is available free of charge at https://pubs.acs.org/doi/10.1021/acs.analchem.1c00976.

DNA sequences; TEM, XRD, XPS spectra of the ZIF materials; and additional fluorescence-based selectivity data (PDF)

AUTHOR INFORMATION

Corresponding Authors

Gang Xie − *Key Laboratory of Synthetic and Natural Functional Molecule Chemistry of Ministry of Education, College of Chemistry & Materials Science, Northwest University, Xi'an, Shaanxi 710127, China*; Email: xiegang@nwu.edu.cn

Juewen Liu − *Department of Chemistry, Waterloo Institute for Nanotechnology, University of Waterloo, Waterloo, Ontario N2L 3G1, Canada*; orcid.org/0000-0001-5918-9336; Email: liujw@uwaterloo.ca

Authors

Zhen Wang − *Key Laboratory of Synthetic and Natural Functional Molecule Chemistry of Ministry of Education, College of Chemistry & Materials Science, Northwest University, Xi'an, Shaanxi 710127, China; Department of Chemistry, Waterloo Institute for Nanotechnology, University of Waterloo, Waterloo, Ontario N2L 3G1, Canada*

Xumei Zhou − *Key Laboratory of Synthetic and Natural Functional Molecule Chemistry of Ministry of Education, College of Chemistry & Materials Science, Northwest University, Xi'an, Shaanxi 710127, China*

Yuqing Li − *Department of Chemistry, Waterloo Institute for Nanotechnology, University of Waterloo, Waterloo, Ontario N2L 3G1, Canada*

Zhicheng Huang − *Department of Chemistry, Waterloo Institute for Nanotechnology, University of Waterloo, Waterloo, Ontario N2L 3G1, Canada*

Jing Han − *Key Laboratory of Synthetic and Natural Functional Molecule Chemistry of Ministry of Education, College of Chemistry & Materials Science, Northwest University, Xi'an, Shaanxi 710127, China*

Complete contact information is available at: https://pubs.acs.org/10.1021/acs.analchem.1c00976

Notes

The authors declare no competing financial interest.

ACKNOWLEDGMENTS

Funding for this work was from the Natural Sciences and Engineering Research Council of Canada (NSERC). Z.W. was supported by a China Scholarship Council Scholarship to visit the University of Waterloo.

REFERENCES

(1) Chinen, A. B.; Guan, C. M.; Ferrer, J. R.; Barnaby, S. N.; Merkel, T. J.; Mirkin, C. A. *Chem. Rev.* **2015**, *115*, 10530−10574.

(2) Yang, F.; Zuo, X.; Fan, C.; Zhang, X.-E. *Natl. Sci. Rev.* **2018**, *5*, 740−755.

(3) Lin, Y.; Yang, Z.; Lake, R. J.; Zheng, C.; Lu, Y. *Angew. Chem., Int. Ed.* **2019**, *58*, 17061−17067.

(4) Liu, B.; Liu, J. *Matter* **2019**, *1*, 825−847.

(5) Liu, B.; Liu, J. *Chem. Commun.* **2014**, *50*, 8568−8570.

(6) Liu, B.; Sun, Z.; Huang, P.-J. J.; Liu, J. *J. Am. Chem. Soc.* **2015**, *137*, 1290−1295.

(7) Yuan, S.; Feng, L.; Wang, K.; Pang, J.; Bosch, M.; Lollar, C.; Sun, Y.; Qin, J.; Yang, X.; Zhang, P.; Wang, Q.; Zou, L.; Zhang, Y.; Zhang, L.; Fang, Y.; Li, J.; Zhou, H.-C. *Adv. Mater.* **2018**, *30*, 1704303.

(8) Hu, X.; Liu, X.; Chen, K.; Wang, G.; Wang, H. *J. Mater. Chem. A* **2019**, *7*, 11016−11037.

(9) Zhang, H.; Hao, C.; Qu, A.; Sun, M.; Xu, L.; Xu, C.; Kuang, H. *Adv. Funct. Mater.* **2018**, *28*, 1805320.

(10) Chen, W.-H.; Luo, G.-F.; Vázquez-González, M.; Cazelles, R.; Sohn, Y. S.; Nechushtai, R.; Mandel, Y.; Willner, I. *ACS Nano* **2018**, *12*, 7538−7545.

(11) Guan, B. Y.; Yu, X. Y.; Wu, H. B.; Lou, X. W. D. *Adv. Mater.* **2017**, *29*, 1703614.

(12) Kuo, C.-H.; Tang, Y.; Chou, L.-Y.; Sneed, B. T.; Brodsky, C. N.; Zhao, Z.; Tsung, C.-K. *J. Am. Chem. Soc.* **2012**, *134*, 14345−14348.

(13) Fang, Y.; Wang, H.-M.; Gu, Y.-X.; Yu, L.; Wang, A.-J.; Yuan, P.-X.; Feng, J.-J. *Anal. Chem.* **2020**, *92*, 3206−3212.

(14) Lu, L.; Si, J. C.; Gao, Z. F.; Zhang, Y.; Lei, J. L.; Luo, H. Q.; Li, N. B. *Biosens. Bioelectron.* **2015**, *63*, 14−20.
(15) Liu, Y.; Lei, J.; Huang, Y.; Ju, H. *Anal. Chem.* **2014**, *86*, 8735−8741.
(16) Wu, C.; Wang, S.; Luo, X.; Yuan, R.; Yang, X. *Chem. Commun.* **2020**, *56*, 1413−1416.
(17) Chen, C.; Zhao, D.; Jiang, Y.; Ni, P.; Zhang, C.; Wang, B.; Yang, F.; Lu, Y.; Sun, J. *Anal. Chem.* **2019**, *91*, 15017−15024.
(18) Wang, L.; Yuan, L.; Zeng, X.; Peng, J.; Ni, Y.; Er, J. C.; Xu, W.; Agrawalla, B. K.; Su, D.; Kim, B.; Chang, Y.-T. *Angew. Chem., Int. Ed.* **2016**, *128*, 1805−1808.
(19) Wang, X.; Qin, L.; Lin, M.; Xing, H.; Wei, H. *Anal. Chem.* **2019**, *91*, 10648−10656.
(20) Wang, M.; Yang, L.; Hu, B.; Liu, J.; He, L.; Jia, Q.; Song, Y.; Zhang, Z. *Biosens. Bioelectron.* **2018**, *113*, 16−24.
(21) Huo, Y.; Qi, L.; Lv, X.-J.; Lai, T.; Zhang, J.; Zhang, Z.-Q. *Biosens. Bioelectron.* **2016**, *78*, 315−320.
(22) Sun, S.; Jiang, K.; Qian, S.; Wang, Y.; Lin, H. *Anal. Chem.* **2017**, *89*, 5542−5548.
(23) Zhong, Y.; Yi, T. *J. Mater. Chem. B* **2019**, *7*, 2549−2556.
(24) Sassanfar, M.; Szostak, J. W. *Nature* **1993**, *364*, 550−553.
(25) Lee, H. N.; Xu, Z.; Kim, S. K.; Swamy, K. M. K.; Kim, Y.; Kim, S.-J.; Yoon, J. *J. Am. Chem. Soc.* **2007**, *129*, 3828−3829.
(26) Das, S.; Sarkar, H. S.; Uddin, M. R.; Rissanen, K.; Mandal, S.; Sahoo, P. *Chem. Commun.* **2019**, *55*, 13016.
(27) Du, T.; Zhao, C.; Rehman, F.; Lai, L.; Li, X.; Sun, Y.; Luo, S.; Jiang, H.; Gu, N.; Selke, M.; Wang, X. *Adv. Funct. Mater.* **2017**, *27*, 1603926.
(28) Liu, B.; Wu, P.; Huang, Z.; Ma, L.; Liu, J. *J. Am. Chem. Soc.* **2018**, *140*, 4499−4502.
(29) Park, J. S.; Na, H.-K.; Min, D.-H.; Kim, D.-E. *Analyst* **2013**, *138*, 1745−1749.
(30) Pautler, R.; Kelly, E. Y.; Huang, P.-J. J.; Cao, J.; Liu, B.; Liu, J. *ACS Appl. Mater. Interfaces* **2013**, *5*, 6820−6825.
(31) Wang, X.; Lopez, A.; Liu, J. *Langmuir* **2018**, *34*, 7899−7905.
(32) Ma, L.; Liu, B.; Huang, P.-J. J.; Zhang, X.; Liu, J. *Langmuir* **2016**, *32*, 5672−5680.
(33) Li, Y.; Zhang, Z.; Liu, B.; Liu, J. *ACS Appl. Bio Mater.* **2019**, *3*, 2568−2576.
(34) Zhang, F.; Huang, P.-J. J.; Liu, J. *ACS Sens.* **2020**, *5*, 2885−2893.
(35) Huizenga, D. E.; Szostak, J. W. *Biochemistry* **1995**, *34*, 656−665.
(36) Li, Y.; Liu, J. *Analyst* **2020**, *145*, 6753−6768.
(37) Wang, Y.; Li, Z.; Hu, D.; Lin, C.-T.; Li, J.; Lin, Y. *J. Am. Chem. Soc.* **2010**, *132*, 9274−9276.
(38) Lu, C.-H.; Yang, H.-H.; Zhu, C.-L.; Chen, X.; Chen, G.-N. *Angew. Chem., Int. Ed.* **2009**, *48*, 4785−4787.
(39) Babu, E.; Muthu Mareeswaran, P.; Ramdass, A.; Ramesh, P.; Rajagopal, S. *J. Lumin.* **2016**, *175*, 267−273.
(40) Bansal, D.; Gupta, R. *Dalton Trans.* **2019**, *48*, 14737−14747.
(41) Wen, J.; Geng, Z.; Yin, Y.; Zhang, Z.; Wang, Z. *Dalton Trans.* **2011**, *40*, 1984−1989.
(42) Rao, A.; Kim, D.; Nam, H.; Jo, H.; Kim, K.; Ban, C.; Ahn, K. *Chem. Commun.* **2012**, *48*, 3206−3208.
(43) Strianese, M.; Milione, S.; Maranzana, A.; Grassi, A.; Pellecchia, C. *Chem. Commun.* **2012**, *48*, 11419−11421.
(44) Hewitt, S. H.; Parris, J.; Mailhot, R.; Butler, S. J. *Chem. Commun.* **2017**, *53*, 12626−12629.
(45) Zwicker, V. E.; Sergeant, G. E.; New, E. J.; Jolliffe, K. A. *Org. Biomol. Chem.* **2021**, *19*, 1017−1021.
(46) Pierce, M. M.; Raman, C. S.; Nall, B. T. *Methods* **1999**, *19*, 213−221.
(47) Li, Y.; Liu, B.; Huang, Z.; Liu, J. *Chem. Sci.* **2020**, *11*, 2735−2743.
(48) Holbrook, J. A.; Capp, M. W.; Saecker, R. M.; Record, M. T. *Biochemistry* **1999**, *38*, 8409−8422.
(49) Gourishankar, A.; Shukla, S.; Ganesh, K. N.; Sastry, M. *J. Am. Chem. Soc.* **2004**, *126*, 13186−13187.
(50) Varghese, N.; Mogera, U.; Govindaraj, A.; Das, A.; Maiti, P. K.; Sood, A. K.; Rao, C. N. R. *ChemPhysChem* **2009**, *10*, 206−210.
(51) Nutiu, R.; Li, Y. *J. Am. Chem. Soc.* **2003**, *125*, 4771−4778.
(52) Xiang, Y.; Wang, Z.; Xing, H.; Wong, N. Y.; Lu, Y. *Anal. Chem.* **2010**, *82*, 4122−4129.

https://doi.org/10.1021/acs.analchem.1c00976
Anal. Chem. 2021, 93, 7707−7713